Application of Advanced Computational Modelling in the Numerical Prediction of the Haemodynamic Impact of Coronary Stent Implantation

JONATHAN MURPHY, FERGAL BOYLE
Department of Mechanical Engineering
Dublin Institute of Technology
Bolton Street, Dublin 1
IRELAND

Abstract: Coronary stent implantation can improve blood flow in an artery narrowed by the build up of arterial plaque. However, the haemodynamic effect of stent placement is unclear and may influence arterial restenosis (re-blockage). In this investigation the stent induced, non-Newtonian blood flow disturbances have been captured in a three dimensional computational domain. The results clearly show areas of low wall shear stress proximal and distal to the stent wires, a characteristic which is known to encourage restenosis. Furthermore, this computational method of observing the complex haemodynamics of the stent environment can be used in conjunction with medical trial data to find links between stent design and restenosis patterns.

Key–Words: Coronary Stent, Computational Fluid Dynamics, Restenosis, Shear Stress, Non-Newtonian Flow Model, Stent Design.

1. Introduction

Coronary artery disease (CAD) is one of the leading causes of death in the developed world. CAD occurs due to the build up of plaque in the coronary arteries which supply fresh blood to the constantly active heart muscle. This build up of plaque, a condition known as atherosclerosis, deprives the heart muscle of its crucial supply of oxygen and nutrients provided by the coronary blood supply. In the past a coronary artery bypass graft was the only treatment available for CAD. This is a large scale operation involving the sawing open of the breastbone and grafting of a blood vessel to bypass the site of the blockage.

Percutaneous transluminal coronary angioplasty (PTCA) was introduced in the late 1970s as a non-surgical procedure to relieve a narrowing in a coronary artery. PTCA is accomplished with a small balloon catheter inserted into an artery in the groin or arm, and advanced to the narrowing in the coronary artery. The balloon is then inflated to enlarge the narrowing in the artery and restore blood flow to the heart muscle. However in over 40% of cases the artery is re-blocked within six months; a process known as restenosis [1]. This is largely due to elastic recoil of the vessel wall [2].

In the early 1990s stents were introduced to improve the success rates of PTCA. Basically, a stent is an expandable, slotted metal tube, inserted into the artery. It acts as a scaffold to provide support for the artery and has proven effective at eliminating elastic recoil, one mechanism of restenosis that can result in re-blockage [2]. The use of stents has shown more promising clinical outcomes than PTCA alone. However, restenosis remains a persistent problem with rates still as high as 20% at six months after intervention [3].

The flow disturbances induced by an implanted stent play a significant role in the immunological behaviour of the coronary artery. This behaviour is directly linked to restenosis within the stented artery [4, 5]. In order to assess the haemodynamic impact of coronary stent implantation, a three-dimensional computational model of a left anterior descending (LAD) coronary artery with an implanted Palmaz-Schatz stent has been created using computer-aided-design. Computational fluid dynamics (CFD) was used to simulate the flow field of the coronary artery with the implanted stent. The results show the mesh convergence study and contour plots of areas of high and low wall shear stress (WSS) around the stent.

2. Stents

2.1 Introduction

Stents are small tubular prostheses that serve the purpose of maintaining an adequate inner diameter of a narrowed blood vessel to allow for the comfortable passage of the blood. In 1986 Jacques Puel and

Ulrich Sigwart implanted the first coronary wallstents in Toulouse, France. Today over 1 million stents are implanted worldwide each year.
A stent is mounted on a balloon-tipped catheter, threaded through the artery, and positioned at the blockage. As shown in Figure 1 the balloon is then inflated, opening the stent. Subsequently, the catheter and deflated balloon are removed, leaving the stent lodged in place against the inner lining of the artery.

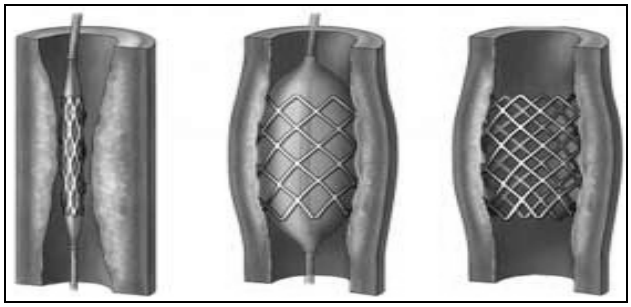

Fig. 1: The stenting procedure for a narrowed artery.

2.2 Stent Design

Two stent designs are shown in Figures 2 and 3 below. The first is the Palmaz-Schatz coronary stent manufactured by Johnson and Johnson. The stent is 15 mm long, consisting of two 7 mm sections joined by a 1 mm bridge. It ranges from 3 mm to 4 mm in diameter and is a slotted tube balloon expandable design. The second type of design is the Gianturco-Roubin II (GRII) stent manufactured by Cook. The GRII stent has a balloon expandable coil design and is produced in 20 mm and 40 mm lengths ranging from 2.5 mm to 4 mm in diameter.

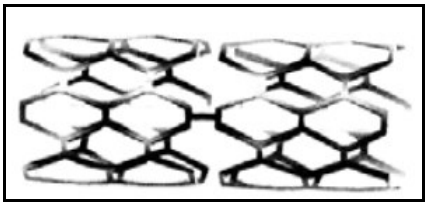

Fig. 2: The Palmaz-Schatz coronary stent.

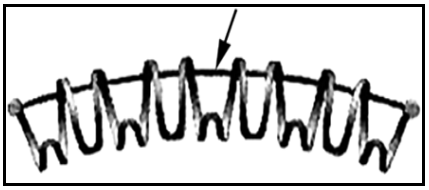

Fig. 3: The Gianturco-Roubin II coronary stent.

2.3 Mechanism of Stent Restenosis

The implantation of a coronary stent leads to an immunological response from the coronary artery which may result in restenosis. Under normal healthy conditions vascular smooth muscle cells (VSMC) reside in the lunica media which is shown in the arterial cross section in Figure 4. Stent restenosis occurs when VSMC migrate through the lunica intima which is the inner lining of the artery wall, and build up in the artery lumen restricting the blood flow, a process known as neointimal hyperplasia (NH). The main components of the coronary artery that determine the degree of restenosis that will occur are the blood clotting platelets which flow through the artery lumen and the endothelial cells (EC) which form the lunica intima.

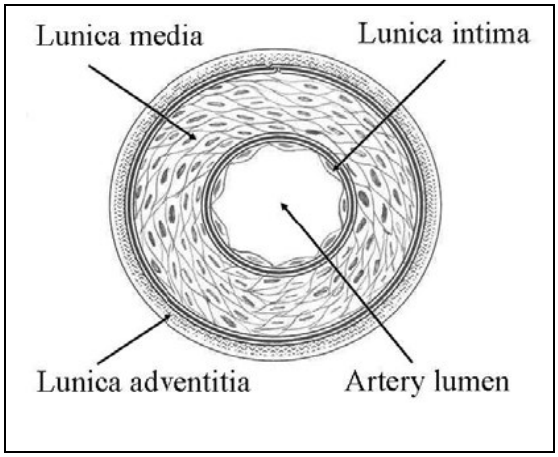

Fig 4: Cross section of a coronary artery.

Platelets flowing in the artery lumen will bind together to form a blood clot if they become activated. Platelets can be activated through contact with a number of different substances such as thrombin or platelet derived growth factor (PDGF). Activated platelets will themselves release these substances to activate platelets around them. However, PDGF also has the effect of triggering NH. It has been documented that the platelet deposition near the stent in the first twelve hours after stenting is a major indicator of the amount of NH that will occur [6].
Platelets and endothelial cells are directly affected by the shear force exerted by the flowing blood on the artery lumen wall known as WSS. It has been shown in a two-dimensional CFD study that areas of low velocity flow and low WSS exist in the vicinity of newly implanted stent wires [7]. The platelet deposition and residence times are much higher in these stagnation areas. This leads to platelet accumulation in the area around the stent wire leading to increased NH formation. The stent induced changes in the haemodynamics of the coronary flow also lead to an alteration of the WSS exerted on the EC [5]. WSS has been shown to have a significant effect on the behaviour of EC [9]. A healthy value for WSS in a coronary artery is approximately 1.5 Pascals [10]. When EC are subjected to values of WSS lower than this they begin to release adenosine

diphosphate and triphosphate which induces platelet activation leading to blood clotting and NH formation [9]. Conversely, when endothelial cells are subjected to areas of "healthy" WSS they secrete nitrous oxide (NO) which inhibits adhesion of platelets to the vessel wall and VSMC growth, hence inhibiting NH formation [10]. Numerous studies have shown a link between areas of low WSS and increased NH [4, 5, 8].

The success of a stenting procedure relies heavily on the reendothelialisation of the vessel wall after implantation and the successful function of the newly formed endothelial cells to inhibit platelet deposition. If a new layer of EC successfully grows over the stent the NH formation will cease. In a study to demonstrate the effect of wall shear stress gradients (WSSG), EC were exposed to a region of separated flow. After 48 hours the major finding was that in the area of the highest WSSG the EC density was up to 40% less than experimental controls [11]. Through the inhibition of reendothelialisation, high WSSG contribute to NH formation [5].

EC will be damaged by the stenting procedure leading to the release of platelet activating substances and NH formation. A relationship has been established between vascular injury and NH [12].

Areas of low WSS, areas of high WSSG, and vascular injury at the time of stent implantation are the main contributors to NH formation. In light of this, disturbances to the coronary blood flow and the degree of trauma to the vessel wall due to stent implantation cannot be overlooked in future stent design.

3. CFD Analysis

3.1 Introduction

CFD is a process whereby real-life fluid flows are simulated using numerical methods to solve the governing equations of fluid dynamics. CFD is a relatively new branch of fluid dynamics commonly regarded as the "third" technique for solution of fluid flow problems, complementing, but not replacing the well-established approaches of theory and experiment. CFD finds it niche in modelling fluid flows that are difficult or impossible to model using theory and are complex, time consuming or expensive to measure experimentally.

3.2 The Computational Model

The computational model shown in Figure 5 represents one of the 7 mm sections of the Palmaz-Schatz stent semi-embedded in the LAD coronary artery. The 3 mm diameter Palmaz-Schatz stent configuration is cut from a 2.94 mm diameter cylindrical domain to simulate these conditions. The domain extends 2.5 mm proximal (upstream) and 2.5 mm distal (downstream) to the stented section to capture the flow field in those regions.

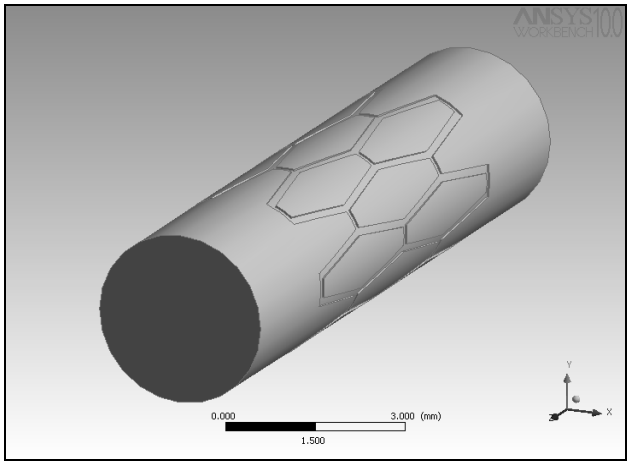

Fig. 5: Computational domain representing the left anterior descending coronary artery with implanted Palmaz-Schatz stent.

3.3 Governing Equations of Fluid Mechanics

This simulation involves steady laminar flow which requires the CFD code to solve the conservation of mass and momentum equations, the general form of the governing equations of fluid mechanics are listed as Equations (1) and (2) respectively:

$$\frac{\partial \rho}{\partial t} + \nabla.\left(\rho \vec{V}\right) = 0 \quad (1)$$

$$\frac{\partial \rho \vec{V}}{\partial t} + \nabla.\left(\rho \vec{V} \otimes \vec{V}\right) = -\vec{\nabla} p + \vec{\nabla}.(\tau) + \rho \vec{g} + \vec{F} \quad (2)$$

where ρ is the fluid density, p is the static pressure, $\vec{V}$ is the velocity vector, $\vec{F}$ represents external body forces such as gravity, μ is the fluid viscosity and τ is the shear stress tensor given by Equation (3):

$$\tau = \mu\left(\nabla \vec{V} + \nabla \vec{V}^{T}\right) \quad (3)$$

At low shear rates blood exhibits the non-Newtonian behaviour of variable viscosity which is dependant on the shear rate. The non-Newtonian nature of the flow is accommodated by using the Carreau model [13] given in Equation (4):

$$\mu = \mu_{\infty} + (\mu_0 - \mu_{\infty})\left[1 + (\gamma\lambda)^2\right]^{\left(\frac{q-1}{2}\right)} \quad (4)$$

where γ is the rate of deformation tensor given by Equation (5) in a three-dimensional Cartesian coordinate system

$$\gamma = \left[\begin{array}{l} 2\left\{ \left(\frac{\partial v_x}{\partial x}\right)^2 + \left(\frac{\partial v_y}{\partial y}\right)^2 + \left(\frac{\partial v_z}{\partial z}\right)^2 \right\} \\ + \left(\frac{\partial v_x}{\partial y} + \frac{\partial v_y}{\partial x}\right)^2 + \left(\frac{\partial v_x}{\partial z} + \frac{\partial v_z}{\partial x}\right)^2 + \left(\frac{\partial v_y}{\partial z} + \frac{\partial v_z}{\partial y}\right)^2 \end{array} \right]^{\frac{1}{2}} \quad (5)$$

and the constants for the Carreau model in Equation (6) have been established from experimental data [13]:

$$\begin{array}{ll} \mu_0 = 0.056 \text{ Pa.s} & \lambda = 3.31 \text{ s} \\ \mu_\infty = 0.00345 \text{ Pa.s} & q = 0.375 \end{array} \quad (6)$$

The highly sophisticated commercial software code CFX™ is used to solve the governing equations of fluid mechanics for non-Newtonian blood flow in the vicinity of the implanted stent using a vertex-centred finite volume scheme.

3.4 Boundary Conditions

3.4.1 Inlet

A fully developed axial velocity profile is applied at the inlet given by:

$$V = V_{Max}\left(1 - \frac{r^2}{R^2}\right) \quad (7)$$

where the variable r is the radius measured from the centreline at any point on the inlet plane and R is the radius at the wall of the domain. V_{Max} is the maximum centreline velocity given a value of 0.412 m/s in Equation (7) to simulate resting conditions in the LAD coronary artery [14].

3.4.2 Outlet

A static pressure of zero Pascals was applied at the outlet of the domain to allow the software to calculate the velocity at this plane.

3.4.3 Wall

The no-slip boundary condition was applied on all surfaces representative of the artery wall and the stent wires.

3.5 Computational Mesh

Analytical solutions to the governing equations of fluid mechanics exist for only the simplest of flows under ideal conditions. To obtain solutions for real flows a numerical approach must be adopted whereby the equations are replaced by algebraic approximations which may be solved using a numerical method. To achieve this, the computational domain must be divided into a set of much smaller non-overlapping sub-domains called elements which constitute the mesh. To obtain an accurate solution a sufficient number of elements must be placed in areas of interest where the nature of the flow changes rapidly. Figure 6 shows the fine mesh employed in the area around the stent wires.

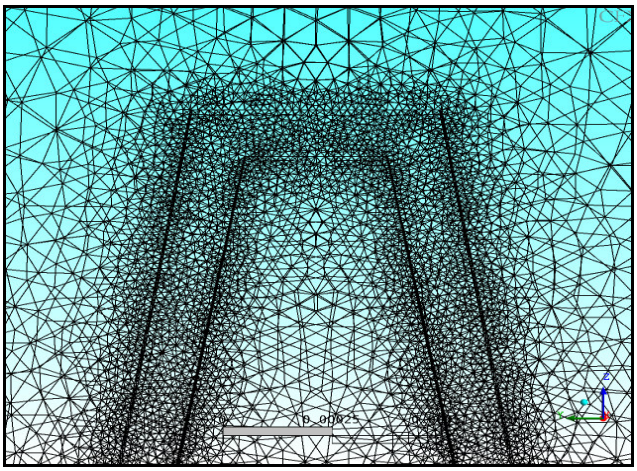

Fig. 6: Computational mesh in the vicinity of a stent strut.

4. Results

4.1 Mesh Convergence Study

A mesh convergence study was carried out to establish the required mesh density for accurate solutions, such that any increase in nodes would lead to no appreciable difference in the solution. Mesh convergence was achieved by sequentially increasing the number of nodes until there was no appreciable difference in the axial distribution of WSS across one of the stent struts between the solutions. A total of 975,613 nodes were used in the final mesh.

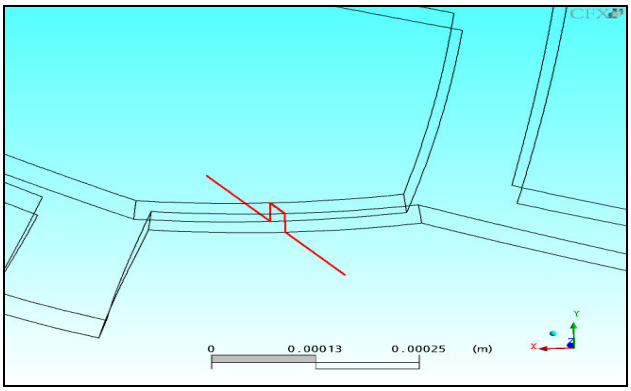

Fig. 7: Stent strut and sample line upon which mesh convergence study was carried out.

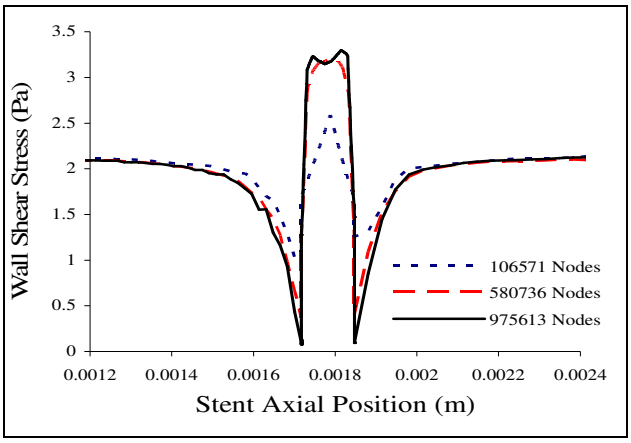

Fig. 8: Axial distributions of wall shear stress across stent strut as calculated by successively refined computational meshes.

4.2 Wall Shear Stress Results

The predicted three-dimensional flow field reveals areas of high WSS on the tops of the stent struts and low WSS immediately proximal and distal to the stent struts, particularly those transversal to the blood flow as shown in Figure 9.

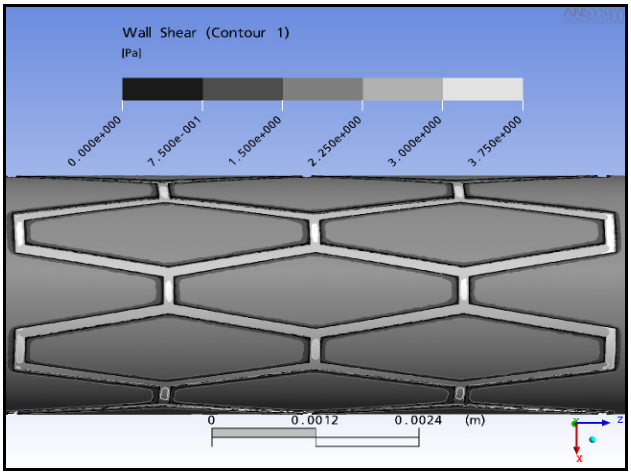

Fig. 9: Contour map of wall shear stress in the vicinity of the implanted Palmaz-Schatz coronary stent.

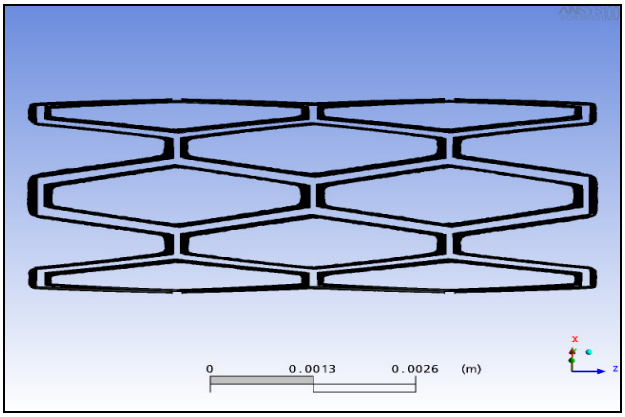

Fig. 10: Highlighted region of WSS with a magnitude of between 0 and 1.5 Pascals in the vicinity of the stent.

Regions of WSS with a magnitude of less than 1.5 Pascals have been identified to be susceptible to NH [10]. Figure 10 illustrates the area in the vicinity of the stent where WSS of a value between 0 and 1.5 Pascals exists. The area of the stented artery subjected to WSS in this range is 12.6 mm^2 or 14.2 % of the total stented area.

A relationship between high WSSG and reduced endothelial growth has been established [11]. Regions of high WSS exist at the tops of stent struts producing large WSS gradients as shown in Figure 9. This has been shown to lead to an area of low density endothelial cell growth which would encourage restenosis.

5. Conclusion

It is clear that haemodynamics of the flow in an artery implanted with a stent have an effect on the immunological response within the vessel wall of that artery. This work has demonstrated that stent design has an effect on those haemodynamic characteristics.

The results presented here have highlighted areas of low WSS and high WSSG. It is also predicted that 14.2 % of the stented region of the artery is subjected to an area of WSS below a healthy threshold of 1.5 Pascals. This quantitative analysis can be used to compare different stent designs from a haemodynamic perspective.

In ongoing research the author is creating a CFD model of blood flow through the LAD coronary artery implanted with a GR II stent which has a record of poor medical performance and is shown in Figure 3. The GR II stent will be tested using the same methodology outlined in this paper and the flow field will be compared to that of the Palmaz-Schatz results.

This work has demonstrated the ability of applied computer science to provide the biomedical community with insights into complex haemodynamics that can be used to assist in the development of optimal stent designs for the future.

Acknowledgements

This study has been funded by the Dept. of Mechanical Engineering, DIT, and also by the Embark Initiative managed by the IRCSET as part of the National Development Plan, Ireland 2000 - 2006.

References

[1] Fischman, D. L., Leon, M. B., and Baim, D. S., A Randomized Comparison of Coronary Stent Placement and Balloon Angioplasty in Treatment of Coronary Artery Disease, *New*

England Journal of Medicine, Vol. 331, 1994, pp. 496-501.

[2] Haude, M., Erbel, R., Issa, H., and Meyer, J., Quantitative Analysis of Elastic Recoil After Balloon Angioplasty and After Intracoronary Implantation of Balloon-Expandable Palmaz-Schatz Stents, *Journal of the American College of Cardiology,* Vol. 21, No. 1, 1993, pp. 26-34.

[3] Serruys, P. W., De Jaegere, P., and Kiemeneij, F., Comparison of Balloon-Expandable-Stent Implantation with Balloon Angioplasty in Patients with Coronary Heart Disease, *New England Journal of Medicine,* Vol. 331, 1994, pp. 489-495.

[4] Garasic, J., Elazer, E. R., Squire, J. C., Seifert, P., Williams, M., and Rogers, C., Stent and Artery Geometry Determine Intimal Thickening Independent of Arterial Injury, *Circulation,* Vol. 101, 2000, pp. 812-818.

[5] LaDisa, J. F., Olson, L. E., Molthen, R. C., Hettrick, D. A., Pratt, P.F., Hardel, M. D., Kersten, J. R., Warltier, D. C., and Pagel, P. S., Alterations in Wall Shear Stress Predict Sites of Neointimal Hyperplasia After Stent Implantation in Rabbit Iliac Arteries, *American Journal of Physiology,* Vol. 288, 2005, pp. H2465-H2475.

[6] Unterberg, C., Sandrock, D., and Klaus, N., Reduced Acute Thrombus Formation Results in Decreased Neointimal Proliferation After Coronary Angioplasty, *Journal of the American College of Cardiology,* Vol. 26, No. 7, 1995, pp. 1747-1754.

[7] Seo, T., Schachter, L., and Barakat, A., Computational Study of Fluid Mechanical Disturbance Induced by Endovascular Stents, *Annals of Biomedical Engineering,* Vol. 33, No. 4, 2005, pp. 444-456.

[8] Wentzel, J. J., Whelan, D., and Van Der Giessen, W., Coronary Stent Implantation Changes 3-D Vessel Geometry and 3-D Shear Stress Distribution, *Journal of Biomechanics*, Vol. 33, 2000, pp. 1287-1295.

[9] Brown C., Morphological, Biochemical, and Functional Changes in Human Platelets Subjected to Shear Stress, *Journal of Laboratory and Clinical Medicine,* Vol. 86, 1975, pp. 462-471.

[10] Malek, A. M., Alper, S. L., and Izumo, S., Hemodynamic Shear Stress and its Role in Atherosclerosis, *Journal of the American Medical Association,* Vol. 282, No. 21, 1999, pp. 2035-2042.

[11] DePaola, N., Gimbrone, M., Davies, P. F., and Dewey, C. F., Vascular Endothelium Responds to Fluid Shear Stress Gradients, *Arteriosclerosis and Thrombosis,* Vol. 12, 1992, pp. 1254-1257.

[12] Rogers, C., and Edelman, E. R., Endovascular Stent Design Dictates Experimental Restenosis and Thrombosis, *Circulation,* Vol. 91, 1995, pp. 2995-3001.

[13] Jung, H., Choi, J. W., and Park, C. G., Asymmetric Flows of Non-Newtonian Fluids in a Symmetric Stenosed Artery, *Korea-Australia Rheology Journal*, Vol. 16, 2004, pp. 101-108.

[14] Waite, *Biofluid Mechanics in Cardiovascular Systems,* McGraw-Hill, 2006.